FABRICATION AND ELECTROCHEMICAL CHARACTERIZATION OF CATHODE MATERIAL $Na_{1.0}Li_{0.05}Mn_{0.6}Ni_{0.3}Al_{0.05}O_2$ FOR SODIUM ION BATTERIES

Tien Phat Doan[1], Van Tuan Nguyen[1], Van Nguyen To[1], Quy Quyen Ngo[1], Trung Son Luong[1], Van Nghia Nguyen[2], Thi Lan Ngo[1,*]

[1]*Faculty of Physics and Chemical Engineering, Le Quy Don Technical University*

[2]*Hanoi Architectural University*

Abstract

Sodium-ion batteries exhibit structural and operational similarities to lithium-ion batteries, and they are increasingly recognized as a viable alternative to lithium-ion batteries. In this context, it is imperative to investigate electrode materials specific to sodium-ion batteries to enhance their capacity, stability, and cost-effectiveness, thereby facilitating their commercialization in the near future. In pursuit of these objectives, this study successfully synthesized $Na_{1.0}Li_{0.05}Mn_{0.6}Ni_{0.3}Al_{0.05}O_2$using a sol-gel method followed by calcination. The resulting material demonstrated a P2 crystal structure and achieved a maximum specific capacity of 142.2 mAh g^{-1} at a discharge current density of 10 mA g^{-1} within the voltage range of 1.5 to 4.1 V. Furthermore, the material exhibited commendable stability, maintaining 89.1% capacity retention after 50 cycles and 76.4% after 100 charge-discharge cycles at a current density of 15 mA g^{-1} within the same voltage range, indicating its potential as a cathode material for sodium-ion batteries.

Keywords: *Sodium ion battery; positive electrode material; sol-gel method.*

1. Introduction

Lithium-ion batteries (LIBs) are integral to contemporary technology, powering a wide array of devices, including mobile phones, laptops, hybrid electric vehicles, and various large-scale applications [1, 2]. Sodium-ion batteries (SIBs), which share a similar structural and operational framework with LIBs, have emerged as a promising alternative due to the abundant availability of sodium resources in the Earth's crust [3-6]. The escalating demand for lithium and other electrode materials has driven LIB production costs to unprecedented levels, thereby accelerating the commercialization of SIBs [5].

The energy storage capacity of SIBs is contingent upon the specific cathode and anode materials employed. Over the past decade, significant advancements have been made in the development of various cathode materials for SIBs, including oxides [7], phosphates/fluorophosphates [8, 9], and Prussian blues [10, 11]. Among these, layered

[*] Corresponding author email: ngothilan@lqdtu.edu.vn

DOI: 10.56651/lqdtu.jst.v2.n02.871.pce

sodium transition metal oxides (Na_xTMO_2, TM-transition metal) have garnered considerable attention due to their diverse compositional range, ease of synthesis, and high specific capacity. Research efforts have concentrated on optimizing Na_xTMO_2 to yield anode materials that exhibit enhanced energy density, structural stability, and cost efficiency. Notably, manganese-based Na_xTMO_2 materials demonstrate superior capacity and redox reversibility. Furthermore, manganese reserves in the Earth's crust are significantly more abundant than those of other transition metals utilized in electrode applications, specifically, 11.3 times more than nickel and 38.1 times more than cobalt [12]. This abundance positions manganese-based Na_xTMO_2 as a sustainable and economically viable option for SIB production, exemplified by materials such as P2-$Na_{0.67}MnO_2$ [13] and the P2-Na-Fe-Mn-O series [14].

To address the challenges associated with phase transformations in manganese-based Na_xTMO_2, various design and modification strategies have been explored. Substituting manganese ions (Mn^{3+}) with alternative cations such as lithium (Li^+) [15, 16], magnesium (Mg^{2+}) [17], zinc (Zn^{2+}) [18], and aluminum (Al^{3+}) [19, 20] has been shown to enhance structural integrity and cycling stability. However, these substitutions often result in diminished specific capacity and energy density. In this study, we focused on synthesizing $Na_{1.0}Li_{0.05}Mn_{0.6}Ni_{0.3}Al_{0.05}O_2$, hereafter referred to as NLMNA, utilizing a sol-gel method followed by calcination to develop anode materials for sodium-ion batteries characterized by high stability and capacity. The material properties were systematically analyzed using X-ray diffraction (XRD), scanning electron microscopy (SEM), energy dispersive X-ray spectroscopy (EDS), and atomic emission spectroscopy (AES). Additionally, the electrochemical performance of the synthesized materials was evaluated through constant current charging and discharging (GCD) methodologies.

2. Experimental details

2.1. Chemicals

Chemicals used in this study include: Sodium carbonate Na_2CO_3 (Sigma-Aldrich), Lithium carbonate Li_2CO_3 (Sigma-Aldrich), Nickel(II) acetate tetrahydrate $Ni(CH_3COO)_2.\ 4H_2O$ (Xilong, China), Manganese(II) acetate tetrahydrate $Mn(CH_3COO)_2.\ 4H_2O$ (Xilong, China), Aluminium nitrate nonahydrate $Al(NO_3)_3.\ 9H_2O$ (Xilong, China), Citric acid monohydrate $C_6H_8O_7.H_2O$ (Xilong, China); Lithium peclorate $LiClO_4$ (Alfa Aesar); Carbon black (Supper P) (Alfa Aesar); Poly vinylidene fluoride (PVDF) (Alfa Aesar); N-metyl-2-pyrrolidon (NMP) (Alfa Aesar); Ethylene cacbonate (EC) (Sigma – Aldrich); Diethyl cacbonate (Sigma – Aldrich). All chemicals employed were of analytical grade and required no further purification.

2.2. Material synthesis

The initial precursor mixture was prepared as follows: take 2.226 g Na_2CO_3 (21.000 mmol); 0.077 g Li_2CO_3 (1.050 mmol); 22.986 g $Ni(CH_3COO)_2.4H_2O$ (12.000 mmol); 5.882 g $Mn(CH_3COO)_2.4H_2O$ (24.000 mmol); 0.750 g $Al(NO_3)_3.9H_2O$ (2 mmol), and 31,521 g $C_6H_8O_7.H_2O$ (150 mmol). The mass of Na_2CO_3 and Li_2CO_3 salts was taken in excess of 5% compared to the required amount to compensate for the sodium and lithium ions evaporated during the thermal decomposition process. The mixture was transferred to a glass beaker, then 100 mL of distilled water was added, and continuous magnetic stirring was carried out at 80°C until gel formation. The gel was then dried at 120°C until xerogel formation. The xerogel was calcined at 400°C for 2 hours, then continued to calcine at 600°C for 2 hours. The mixture was then ground and mixed well before calcining at 950°C for 20 hours. The material fabrication process is shown in Fig. 1.

2.3. Approach for determining characteristics and properties of materials

Characteristics:

The crystal structure of the synthesized material was characterized using XRD analysis conducted on a Bruker D8 X-ray diffraction instrument. The morphological features and compositional analysis of the material were assessed through SEM and EDS, performed on a Hitachi S-4800 high-resolution scanning electron microscope. Additionally, the AES was utilized for further compositional analysis, employing a PerkinElmer AA-800 instrument.

Electrochemical Properties:

In order to evaluate the electrochemical properties of the synthesized material, a working electrode was prepared following a systematic procedure. The electrode material was combined with superconducting carbon (Supper P) and polyvinylidene fluoride (PVDF) in a weight ratio of 80:10:10. Subsequently, a small quantity of N-methyl-2-pyrrolidone (NMP) solvent was introduced, and the mixture was agitated until a homogeneous slurry was obtained. This slurry was then uniformly applied onto a 15 µm thick aluminum foil substrate and subjected to drying at 100°C in a vacuum oven for a duration of 12 hours. Following the drying process, the aluminum foil containing the electrode material was cut into standard-sized electrode plates compatible with CR2032 batteries. The fabrication of the CR2032 sodium-ion battery was conducted within an argon-filled glove box, ensuring that the concentrations of oxygen (O_2) and water (H_2O) remained below 0.1 ppm. The battery assembly comprised a positive electrode constructed from the NLMNA material, a negative electrode composed of metallic sodium, a polypropylene (PP) membrane serving as a separator between the two electrodes, and an

electrolyte consisting of a 1M $NaClO_4$ solution in a 1:1 volumetric mixture of ethylene carbonate and diethylene carbonate (EC/DEC). The electrochemical performance of the NLMNA material was assessed using the GCD method on a NEWARE automatic discharge device.

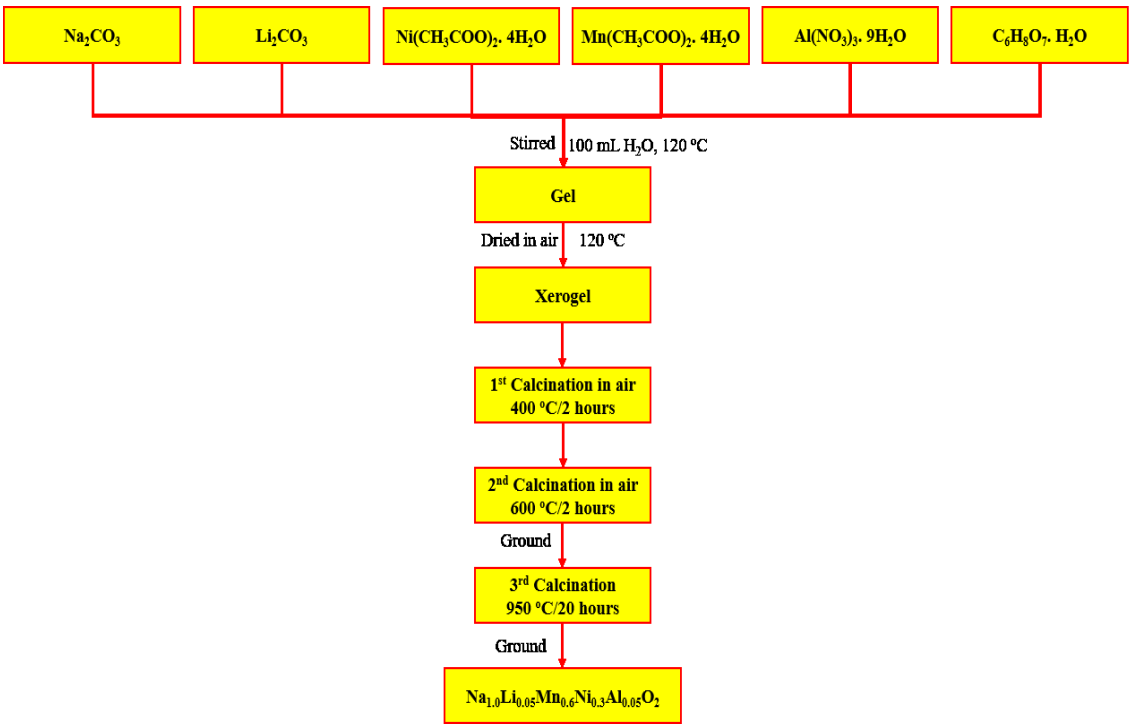

Fig. 1. Material synthesis process of $Na_{1.0}Li_{0.05}Mn_{0.6}Ni_{0.3}Al_{0.05}O_2$.

3. Results and discussion

Figure 2 presents the XRD pattern of the synthesized NLMNA material. The pattern exhibits distinct diffraction peaks at angles of 2θ = 15.9°, 32.2°, 36.0°, 39.7°, 43.5°, 48.9°, 62.4°, 64.3°, and 67.1°. These diffraction peaks agree precisely with the Joint Committee on Powder Diffraction Standards (JCPDS) card #27-0751, which corresponds to a triangular prism structure classified as P2 with a space group of P63/mmc, corroborating findings from prior studies [15, 18, 19, 21]. The sharpness of the diffraction peaks indicates that the synthesized material is free from any impurity phases. Notably, when compared to JCPDS card #27-0751, a diffraction peak corresponding to the (1/3, 1/3, 1) plane is observed at a 2θ angle of 22.3°, suggesting the presence of long-range in-plane ordering between Li and Mn ions [22]. Additionally, three distinct peaks within the 2θ range of 60° to 70° are characteristic of the trigonal prismatic P2 structure, in contrast to the diffraction peaks associated with an orthorhombic P2 structure [23].

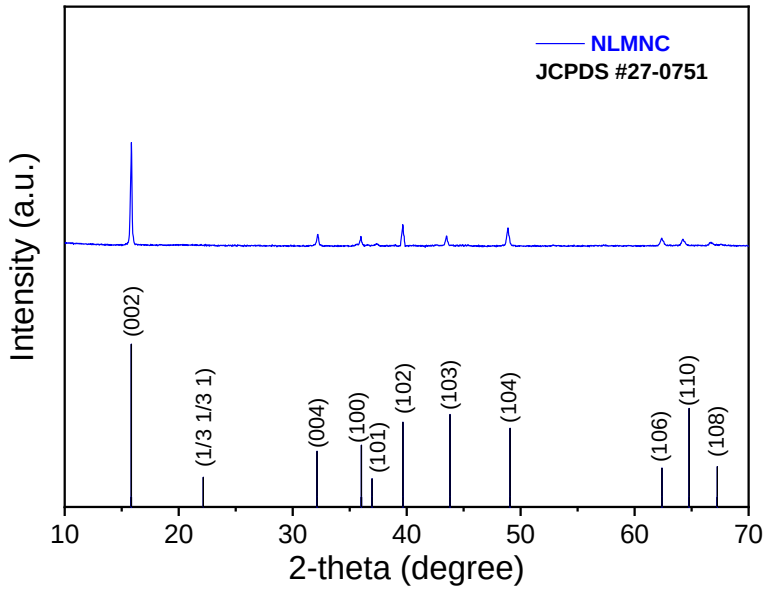

Fig. 2. The XRD pattern of the NLMNA material.

The SEM images of the synthesized NLMNA material are presented in Fig. 3a and 3b. The NLMNA material exhibits a plate-like morphology, with the majority of the plates measuring between 2 and 4 μm in size. This morphological characteristic is consistent with that of P2-$Na_{0.66}Li_{0.18}Fe_{0.12}Mn_{0.7}O_2$ [15] and P2-Na_xMnO_2 [25] materials reported in previous studies. High-resolution SEM image (Fig. 3b) reveals a distinctly layered morphology, with a tendency for the plates to adhere to one another. This phenomenon is attributed to the onset of melting at the surface of the primary particles during the synthesis process at a reaction temperature of 950°C.

The EDS results presented in Fig. 3c confirm the presence of Na, Mn, Ni, Al, and O atoms within the NLMNA material. The absence of Li in the EDS spectrum is due to limitations inherent to the measurement technique, which may not accurately detect light chemical element of Li. The measured atomic ratios of Na, Mn, Ni, and Al are 19.27:18.97:8.99:1.57, which corresponds to a normalized ratio of approximately 0.61:0.60:0.29:0.05. This ratio is relatively close to the intended chemical composition ratio of 1.00:0.60:0.30:0.05 as per the formula $Na_{1.0}Li_{0.05}Mn_{0.6}Ni_{0.3}Al_{0.05}O_2$. The discrepancy in sodium concentration can be attributed to the low sensitivity of EDS for detecting Na.

To ascertain the presence of lithium in the synthesized material, the AES analysis was performed. The analysis indicates a mass ratio of lithium at approximately 0.40%. In comparison, the theoretical mass ratio of lithium in $Na_{1.0}Li_{0.05}Mn_{0.6}Ni_{0.3}Al_{0.05}O_2$ is approximately 0.32%. This observed ratio is consistent with expectations, as both

sodium and lithium may volatilize during high-temperature synthesis, leading to an indeterminate extent of evaporation.

Based on the findings from the XRD, SEM, EDS, and AES analyses, it can be concluded that the material $Na_{1.0}Li_{0.05}Mn_{0.6}Ni_{0.3}Al_{0.05}O_2$ was successfully synthesized with a high purity.

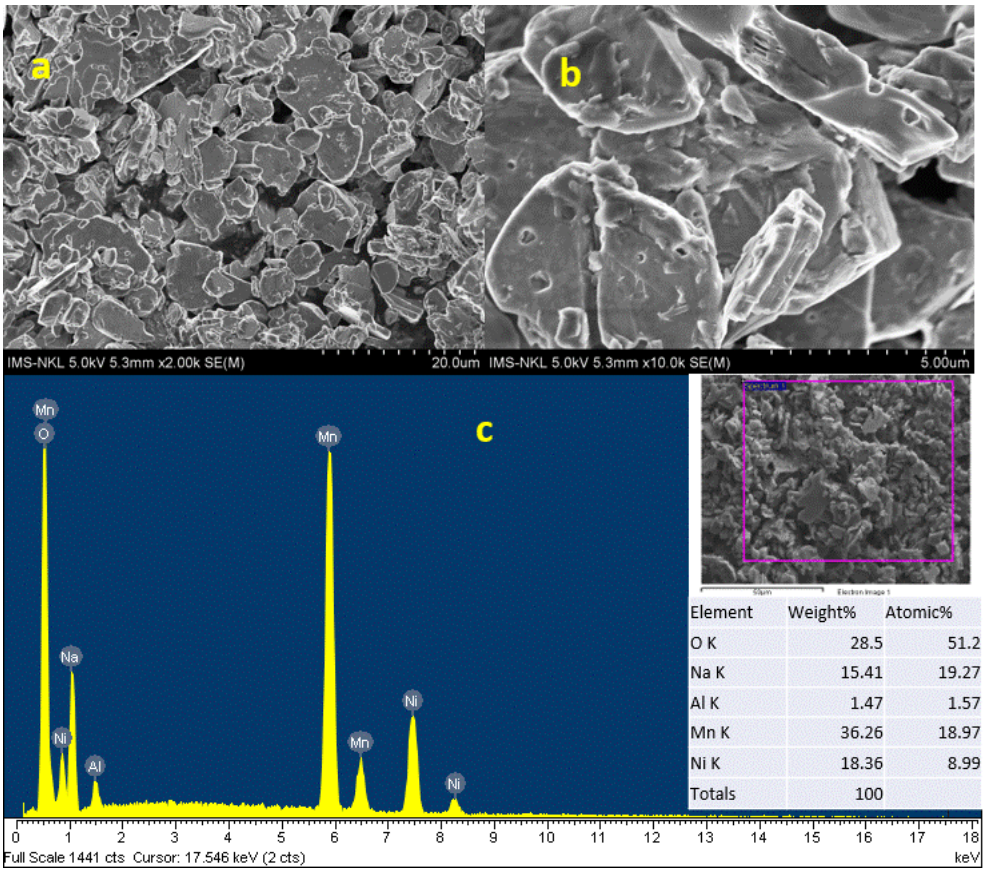

Fig. 3. The SEM morphological images and elemental composion EDS analyses of the synthesized NLMNA material.

The electrochemical properties of the NLMNA material were assessed using the the GCD method. Figure 4(a) illustrates the charge and discharge curves for the initial three cycles at a current density of 10 mA g^{-1}. The specific capacities recorded for these cycles were 137.1 mAh g^{-1}, 136.9 mAh g^{-1}, and 139.6 mAh g^{-1}, respectively. The observed disturbance in the charging curve during the first cycle may be attributed to the instability of the electrode surface structure. However, as the structural stability improves, the diffusion of Na^+ ions becomes more efficient, resulting in an increase in capacity during the initial cycles of the continuous charge-discharge process. This

observation aligns with the results presented in Figures 5a and 5b. As compared to similar materials, such as P2- $Na_{0.75}Li_{0.05}Ni_{0.3}Mn_{0.65}O_2$ which exhibits a capacity of 138 mAh g^{-1} at a current density of 0.1C within a potential range of 1.5 to 4.5 V [24], and $Na_{0.66}Li_{0.18}Fe_{0.12}Mn_{0.7}O_2$ which demonstrates a capacity of 180 mAh g^{-1} at a current density of 10 mA g^{-1} within the same potential range [15], this synthesized NLMNA material displays a relatively high capacity in comparison to these analogous compounds.

To further evaluate the charge and discharge rates of the NLMNA material, the GCD measurements were conducted at varying current densities (10 mA g^{-1}, 20 mA g^{-1}, 30 mA g^{-1}, 50 mA g^{-1}, and 100 mA g^{-1}), with results depicted in Figure 4b. The data indicate that as the current density increases, the specific discharge capacity of the material decreases. This reduction in specific capacity with increasing current density can be attributed to the enhanced efficiency of electrochemical reactions occurring at slower reaction rates within the battery [25].

Figure 4c illustrates the cyclic voltammetry (CV) curve of NLMNA at a scan rate of 0.1 mV/s within the voltage range of 1.5 to 4.1 V. Notably, four pairs of redox peaks are identified between 1.5 and 4.1 V, aligning closely with the four plateaus observed in the charge-discharge curves (Fig. 4a and 4b). The redox peaks at 2.05/1.67 V are associated with the Mn^{2+}/Mn^{3+} redox reaction [26]. Additionally, the peaks at 3.94/3.84 V and 3.60/3.45 V pertain to the continuous reversible conversion of $Ni^{2+}/Ni^{3+}/Ni^{4+}$ [27], while the peaks at 3.23/3.03 V may indicate a phase transition.

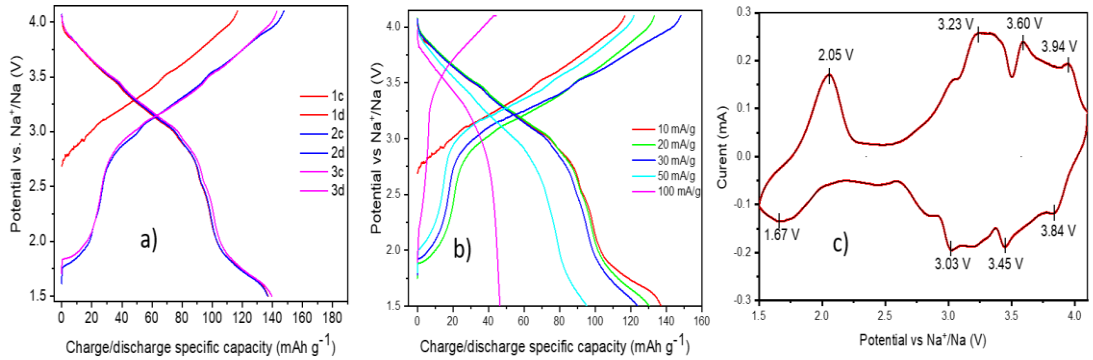

Fig. 4. The GCD curves of NLMNA material: (a) three first cycles at current density 10 mA/g, (b) at different current densities and (c) the cyclic voltammogram of NLNMA.

The repeated charge-discharge measurements were conducted over numerous consecutive cycles at various current densities to assess the stability of the NLMNA

material. The results are illustrated in Fig. 5. Figure 5a presents the specific capacity of the NLMNA material after 35 charge-discharge cycles at current densities of 10, 20, 30, 50, and 100 mA g^{-1}. The obtained results indicate a decline in specific capacity as the current density increases, with recorded specific capacities of 142.2 mAh g^{-1}, 131.6 mAh g^{-1}, 130.5 mAh g^{-1}, 95.4 mAh g^{-1}, and 46.4 mAh g^{-1} for current densities of 10, 20, 30, 50, and 100 mA g^{-1}, respectively. Notably, after completing 25 charge-discharge cycles at increasing current densities and subsequently returning to a current density of 10 mA g^{-1}, the specific capacity exhibited only a minor decrease to 137 mAh g^{-1}. This observation indicates the structural stability of the NLMNA material under high charge-discharge rates. Following 35 continuous charge-discharge cycles at varying current densities, the remaining specific capacity of the NLMNA material was recorded at 131.1 mAh g^{-1}, which corresponds to approximately 95.6% retention of the initial specific capacity. Figure 5b displays the electrochemical performance evaluation after 100 charge-discharge cycles at a fixed current density of 15 mA g^{-1}. The results indicate that after these cycles, the specific capacity remained at 103.64 mAh g^{-1}, equivalent to approximately 76.4% of the initial discharge capacity of 135.65 mAh g^{-1}. Additionally, the coulombic efficiency over these 100 cycles was maintained at approximately 97%. The favorable capacity retention observed after this extensive cycling further demonstrates the stability of the NLMNA material. Comparative analysis with similar materials reveals that the synthesized NLMNA material exhibits commendable cycling stability. Relevant comparative statistics are presented in Table 1.

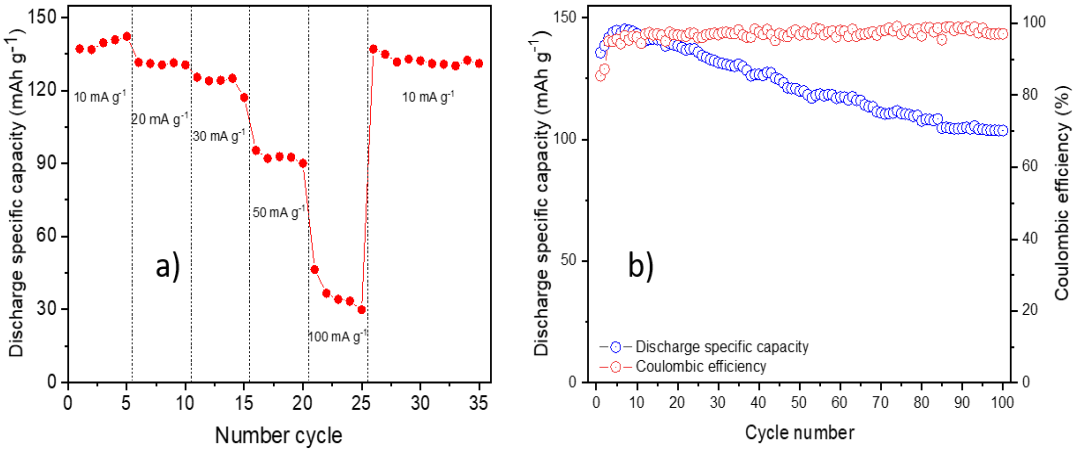

Fig. 5. Cycle performance of NLMNA materials: (a) at different current densities, and (b) at current density of 10 mA g^{-1}.

Table 1. Comparison of cycle performance of NLMNA materials with similar materials

No.	Materials	Specific; remaning capacity	Ref.
1	P2-$Na_{1.0}Li_{0.2}Mn_{0.7}Ti_{0.1}O_2$	146 mAh g^{-1}; 90% after 50 cycles at 0.1C current density, and at 1.5 - 4.0 V voltage range	[21]
2	P2-$Na_{0.66}Li_{0.18}Fe_{0.12}Mn_{0.7}O_2$	190 mAh g^{-1}; 86.8% after 80 cycles at 10 mA g^{-1} current, and in the range of 1.5 - 4.5 V	[15]
3	P2-$Na_{0.95}Li_{0.15}Ni_{0.25}Mn_{0.6}O_2$	140 mAh g^{-1}; 64.6% after 100 cycles at current density of 0.5C, and at 1.8 - 4.2 V voltage range	[24]
4	P2-$Na_{0.67}Mn_{0.8}Fe_{0.18}Al_{0.02}O_2$	139.7 mAh g^{-1}; 78.6% after 100 cycles at current density of 100 mA g^{-1}, and at 2.0 - 4.0 V voltage range	[28]
5	**P2-$Na_{1.0}Li_{0.05}Mn_{0.6}Ni_{0.3}Al_{0.05}O_2$**	142.2 mAh g^{-1}; 89,1% after 50 cycles and 76.4% after 100 cycles at current density of 15 mA g^{-1}, and at 1.5 - 4.1 V voltage range	This work

4. Conclusions

This study successfully synthesized the layered structure material $Na_{1.0}Li_{0.05}Mn_{0.6}Ni_{0.3}Al_{0.05}O_2$ using a sol-gel method combined with calcination. The synthesized material exhibits a P2 crystal structure and a plate-like morphology with an average particle size of approximately 2 - 4 μm. As compared to similar materials, this NLMNA compound demonstrates high specific capacity and stability of achieving a maximum specific capacity of 142.2 mAh/g at a discharge current density of 10 mA/g within the potential range of 1.5 to 4.1 V. Furthermore, the material maintains 89.1% capacity retention after 50 cycles and 76.4% after 100 continuous charge-discharge cycles at a current density of 15 mA/g within the same voltage range of 1.5 to 4.1 V. These results indicate that the layered structure $Na_{1.0}Li_{0.05}Mn_{0.6}Ni_{0.3}Al_{0.05}O_2$ material, synthesized by the sol-gel method combined with calcination, is a promising candidate material for sodium-ion battery applications.

Acknowledgment

This research is funded by Vietnam National Foundation for Science and Technology Development (NAFOSTED) under the grant number NCUD.01-2022.03.

References

[1] M. S. Whittingham, "Lithium batteries and cathode materials", *Chemical Reviews*, Vol. 104, Iss. 10, pp. 4271-4302, 2004. DOI: 10.1021/cr020731c

[2] J. B. Goodenough and Y. Kim, "Challenges for rechargeable Li batteries", *Chemistry of Materials*, Vol. 22, Iss. 3, pp. 587-603, 2010. DOI: 10.1021/cm901452z

[3] C. Vaalma, D. Buchholz, M. Weil, and S. Passerini, "A cost and resource analysis of sodium-ion batteries", *Nature Reviews Materials*, Vol. 3, Iss. 4, pp. 1-11, 2018. DOI: 10.1038/natrevmats.2018.13

[4] N. Yabuuchi, K. Kubota, M. Dahbi, and S. Komaba, "Research development on sodium-ion batteries", *Chemical Reviews*, Vol. 114, Iss. 23, pp. 11636-11682, 2014. DOI: 10.1021/cr500192f

[5] P. K. Nayak, L. Yang, W. Brehm, and P. Adelhelm, "From lithium-ion to sodium-ion batteries: Advantages, challenges, and surprises", *Angewandte Chemie International Edition*, Vol. 57, Iss. 1, pp. 102-120, 2018. DOI: 10.1002/anie.201703772

[6] X. Li, L. Zhao, P. Li, Q. Zhang, and M. S. Wang, "In-situ electron microscopy observation of electrochemical sodium plating and stripping dynamics on carbon nanofiber current collectors", *Nano Energy*, Vol. 42, pp. 122-128, 2017. DOI: 10.1016/j.nanoen.2017.10.050

[7] Y. Wen, J. Fan, C. Shi *et al.*, "Probing into the working mechanism of Mg versus Co in enhancing the electrochemical performance of P2-Type layered composite for sodium-ion batteries", *Nano Energy*, Vol. 60, pp. 162-170, 2019. DOI: 10.1016/j.nanoen.2019.02.074

[8] P. Barpanda, J. Lu, T. Ye, and M. Kajiyama, "A layer-structured $Na_2CoP_2O_7$ pyrophosphate cathode for sodium-ion batteries", *RSC Advances*, Vol. 3, Iss. 12, pp. 3857-3860, 2013. DOI: 10.1039/C3RA23026K

[9] P. Barpanda, T. Ye, S. Nishimura *et al.*, "Sodium iron pyrophosphate: A novel 3.0V iron-based cathode for sodium-ion batteries", *Electrochemistry Communications*, Vol. 24, pp. 116-119, 2012. DOI: 10.1016/j.elecom.2012.08.028

[10] T. Huang, G. Du, Y. Qi *et al.*, "A Prussian blue analogue as a long-life cathode for liquid-state and solid-state sodium-ion batteries", *Inorganic Chemistry Frontier*, Vol. 7, Iss. 20, pp. 3938-3944, 2020. DOI: 10.1039/D0QI00872A

[11] Y. Lu, L. Wang, J. Cheng, and J. B. Goodenough, "Prussian blue: A new framework of electrode materials for sodium batteries", *Chemical Communications*, Vol. 48, Iss. 52, pp. 6544-6546, 2012. DOI: 10.1039/C2CC31777J

[12] C. X. Zu and H. Li, "Thermodynamic analysis on energy densities of batteries", *Energy & Environmental Science*, Vol. 4, Iss. 8, pp. 2614-2624, 2011. DOI: 10.1039/C0EE00777C

[13] S. Kumakura, Y. Tahara, K. Kubota, K. Chihara, and S. Komaba, "Sodium and manganese stoichiometry of P2-type $Na_{2/3}$ MnO_2", *Angewandte Chemie International Edition*, Vol. 55, Iss. 41, pp. 12760-12763, 2016. DOI: 10.1002/anie.201606415

[14] N. Yabuuchi, M. Kajiyama, J. Iwatate *et al.*, "P2-type $Na_x[Fe_{1/2}Mn_{1/2}]O_2$ made from earth-abundant elements for rechargeable Na batteries", *Nature Materials*, Vol. 11, Iss. 6, pp. 512-517, 2012. DOI: 10.1038/nmat3309

[15] L. Yang, X. Li, J. Liu *et al.*, "Lithium-doping stabilized high-performance P2–$Na_{0.66}Li_{0.18}Fe_{0.12}Mn_{0.7}O_2$ cathode for sodium ion batteries", *Journal of the American Chemical Society*, Vol. 141, No. 16, pp. 6680-6689, 2019. DOI: 10.1021/jacs.9b01855

[16] M. S. Kwon, S. G. Lim, Y. Park *et al.*, "P2 orthorhombic $Na_{0.7}[Mn_{1-x}Li_x]O_{2+y}$ as cathode materials for Na-ion batteries", *ACS Applied Materials & Interfaces*, Vol. 9, No. 17, pp. 14758-14768, 2017. DOI: 10.1021/acsami.7b00058

[17] D. Buchholz, C. Vaalma, L. G. Chagas, and S. Passerini, "Mg-doping for improved long-term cyclability of layered Na-ion cathode materials - The example of P2-type $NaxMg_{0.11}Mn_{0.89}O_2$", *Journal of Power Sources*, Vol. 282, pp. 581-585, 2015. DOI: 10.1016/j.jpowsour.2015.02.069

[18] X. Wu, J. Guo, D. Wang *et al.*, "P2-type $Na_{0.6}Ni_{0.33-x}ZnxMn_{0.67}O_2$ as new high-voltage cathode materials for sodium-ion batteries", *Journal of Power Sources*, Vol. 281, pp. 18-26, 2015. DOI: 10.1016/j.jpowsour.2014.12.083

[19] X. Liu, W. Zuo, B. Zheng *et al.*, "P2-$Na_{0.67}Al_xMn_{1-x}O_2$: Cost-effective, stable and high-rate Sodium electrodes by suppressing phase transitions and enhancing sodium cation mobility", *Angewandte Chemie International Edition*, Vol. 58, Iss. 50, pp. 18086-18095, 2019. DOI: 10.1002/anie.201911698

[20] D. Han, J. Ku, R. Kim *et al.*, "Aluminum manganese oxides with mixed crystal structure: High- energy- density cathodes for rechargeable sodium batteries", *ChemSusChem*, Vol. 7, Iss. 7, pp. 1870-1875, 2014. DOI: 10.1002/cssc.201301254

[21] V. N. To, V. K. Nguyen, S. H Nguyen *et al.*, "P2-type layered structure $Na_{1.0}Li_{0.2}Mn_{0.7}Ti_{0.1}O_2$ as a superb electrochemical performance cathode material for sodium-ion batteries", *Journal of Electroanalytical Chemistry*, Vol. 880, 2021. DOI: 10.1016/j.jelechem.2020.114834

[22] N. Yabuuchi, R. Hara, M. Kajiyama *et al.*, "New O2/P2-type Li-excess layered manganese oxides as promising multi-functional electrode materials for rechargeable Li/Na batteries", *Advanced Energy Materials*, Vol. 4, Iss. 13, 2014. DOI: 10.1002/aenm.201301453

[23] D. Su, C. Wang, H. Ahn, and G. Wang, "Single crystalline $Na_{0.7}MnO_2$ nanoplates as cathode materials for sodium- ion batteries with enhanced performance", *Chemistry A European Journal*, Vol. 19, Iss. 33, pp. 10884-10889, 2013. DOI: 10.1002/chem.201301563

[24] L. Li, G. Su, C. Lu *et al.*, "Effect of lithium doping in P2-type layered oxide cathodes on the electrochemical performances of Sodium-ion batteries", *Chemical Engineering Journal*, Vol. 446, 2022. DOI: 10.1016/j.cej.2022.136923

[25] X. Ma, C. Yang, Z. Xu *et al.*, "Structural and electrochemical progress of O3-type layered oxide cathodes for Na-ion batteries", *Nanoscale*, Vol. 15, Iss. 36, pp. 14737-14753, 2023. DOI: 10.1039/D3NR02373G

[26] B. Jiang, J. Li, B. Luo *et al.*, "$LiPO_2F_2$ electrolyte additive for high-performance Li-rich cathode material", *Journal of Energy Chemistry*, Vol. 60, pp. 564-571, 2021. DOI: 10.1016/j.jechem.2021.01.024

[27] L. Yang, S. Luo, Y. Wang *et al.*, "Cu-doped layered P2-type $Na_{0.67}Ni_{0.33-x}Cu_xMn_{0.67}O_2$ cathode electrode material with enhanced electrochemical performance for sodium-ion batteries", *Chemical Engineering Journal*, Vol. 404, 2021. DOI: 10.1016/j.cej.2020.126578

[28] D. Qiao, Y. Zhang, C. Su *et al.*, "Study on the different effects of aluminum doping on Fe-Mn and Ni-Mn based compounds as cathode material for sodium-ion batteries", *Journal of Industrial and Engineering Chemistry*, Vol. 124, pp. 287-293, 2023. DOI: 10.1016/j.jiec.2023.04.019

TỔNG HỢP VÀ NGHIÊN CỨU TÍNH CHẤT ĐIỆN HÓA CỦA VẬT LIỆU ĐIỆN CỰC DƯƠNG $Na_{1,0}Li_{0,05}Mn_{0,6}Ni_{0,3}Al_{0,05}O_2$ DÙNG CHO PIN ION NATRI

Đoàn Tiến Phát[1], Nguyễn Văn Tuấn[1], Tô Văn Nguyện[1], Ngô Quý Quyền[1], Lương Trung Sơn[1], Nguyễn Văn Nghĩa[2], Ngô Thị Lan[1]

[1]*Khoa Hóa - Lý kỹ thuật, Trường Đại học Kỹ thuật Lê Quý Đôn*

[2]*Trường Đại học Kiến trúc Hà Nội*

Tóm tắt: Pin ion natri có cấu tạo và cơ chế hoạt động tương tự như pin ion lithium và đang dần chứng tỏ là giải pháp thay thế lý tưởng cho pin ion natri. Trong bối cảnh đó, cần phải có những nghiên cứu về vật liệu điện cực cho loại pin này nhằm cải thiện dung lượng, tính ổn định và tiết kiệm chi phí sản xuất, để sớm đưa pin ion natri vào thương mại hóa. Với những mục tiêu như trên, trong nghiên cứu này chúng tôi đã tổng hợp thành công vật liệu $Na_{1,0}Li_{0,05}Mn_{0,6}Ni_{0,3}Al_{0,05}O_2$ bằng phương pháp sol-gel kết hợp với nung. Kết quả chỉ ra rằng, vật liệu chế tạo được có cấu trúc P2, đạt dung lượng riêng cao nhất là 142,2 mAh/g với mật độ dòng phóng là 10 mA/g trong khoảng thế 1,5 - 4,1 V; tính ổn định của vật liệu duy trì được 89,1% sau 50 chu kỳ và 76,4% sau 100 chu kỳ nạp xả tại mật độ dòng 15 mA/g trong khoảng thế 1,5 - 4,1 V, hứa hẹn là vật liệu tiềm năng cho sản xuất cực dương cho pin ion natri.

Từ khóa: *Pin ion natri; vật liệu điện cực dương; phương pháp sol-gel.*

Received: 11/09/2024; Revised: 06/10/2024; Accepted for publication: 30/10/2024

❑